

# Texture Analysis and Unsupervised Clustering for Segmenting Iris Images

Asheer K. Bachoo , Jules R. Tapamo

School of Computer Science  
University of KwaZulu-Natal, Durban

{200266744, tapamoj}@ukzn.ac.za

## Abstract

Iris recognition is a relatively new and widely developing technology. The unique and distinct spatial patterns of the iris is used to create a digital signature for person identification. A common problem faced by systems is that of accurate segmentation of the region of interest (ROI). This paper discusses various texture analysis and pattern classification techniques for characterizing the ROI.

## 1. Introduction

The iris begins its formation in the 3<sup>rd</sup> month of gestation [1]. By the 8<sup>th</sup> month, its distinctive pattern is complete. However, pigmentation and even pupil size increase as far up as adolescence [2]. The iris has a multilayered texture. This combination of layers and colour provide a highly distinctive pattern.

Of the utmost importance in a biometric identification system is the stability and uniqueness of the object being analysed. Ophthalmologists [3] and anatomists [4], during the course of clinical observations, have noted that the irises of individuals are highly distinctive. This extends to the left and right eye of the same person. Repeated observations over a period of time have highlighted little variation in the patterns.

Developmental biology has also provided evidence of the particular characteristics of the iris [2]. Although the general structure of the iris is genetically determined, the uniqueness of its minutiae is highly dependent on circumstances. As a result, replication is almost impossible. It has also been noted that, following adolescence, the iris remains stable and varies little for the remainder of the person's life. Development is continuous during the early and adolescent years (pigmentation continues as well as an increase in pupil size) [4, 2].

In 1936, Frank Burch, an ophthalmologist, proposed the idea of using iris patterns for personal identification. However, this was only documented by James Doggarts in 1949. The idea of iris identification for automated recognition was finally patented by Aran Safir and Leonard Flom in 1987. They commissioned John Daugman to develop the fundamental algorithms in 1989. These algorithms were patented by Daugman in 1994 and now form the basis for all current commercial iris recognition systems. The Daugman algorithms are owned by Iridian Technologies and they are licensed to several other companies.

A key part of iris recognition is the segmentation of the iris after an image has been acquired. Current systems rely on a set of assumptions - such as clear boundaries, uncorrupted iris texture and good illumination - that assist with segmentation. However, this is rarely the case and unwanted artifacts present in the image make segmentation a very difficult process.

The fundamental iris recognition papers [5, 6, 7], while instrumental in providing rich knowledge for all subsequent en-

deavors, have not addressed the problem of interference caused by eyelashes, reflection, skin and other artifacts. Iris texture is the ROI and it is required that we remove useless artifacts - such as eyelashes and eyelids - from the iris region. A texture segmentation approach is undertaken.

In this paper we discuss various texture analysis and pattern classification techniques for characterizing the ROI in the segmentation of an iris image. The rest of the paper is organized as follows: in section 2 we present some related work; pre-processing is discussed in section 3; section 4 is devoted to texture analysis; in section 5 we present unsupervised pattern classification; experimental results and discussion are exhibited in section 6; future developments are mentioned in section 7 and in section 8 conclusions are drawn.

## 2. Related Work

The fundamental iris algorithm and system was developed by John Daugman. This was presented in his landmark paper [5] and subsequently updated [8]. The iris is segmented using integro-differential operators. To extract the rich details of the texture, he uses complex-valued 2D Gabor wavelets to extract discriminating information. Recognition is done by means of a test of statistical independence for two iris codes. A failure of the test implies a match. The matching system implements a normalized Hamming distance criteria.

Features can be extracted using an application of Laplacian of Gaussian filters at different resolutions [6]. Feature extraction using zero-crossing representations of a 1D wavelet transform [7], the Haar wavelet [9] and the Haar wavelet with a neural network for identification [10] are well documented. Multi-channel Gabor filtering [11], circular symmetric filters [12] and key local variations in 1D signals [13] have also shown to be very promising for generating digital iris codes.

Images in the real world do not contain uniform intensity. They generally have intensity variations that follow a particular periodicity. This is visual texture [14]. The techniques available for machine learning consist of co-occurrence matrices, Markov random fields, wavelets and fractals, each one being adaptable to a particular situation [15].

An algorithm - void of texture classification - to detect eyelashes for accurate iris segmentation has been proposed in the literature [16]. It divides the problem into two possibilities - separable eyelashes and multiple eyelashes. Separable eyelashes are treated as edges. The image is convolved with a Gabor filter and thresholded to segment the eyelashes. The Gabor function is defined as

$$G(x, u, \sigma) = \exp\left\{-\frac{x^2}{2\sigma^2}\right\} \cos(2\pi ux) \quad (1)$$

where  $u$  is the frequency of the sinusoidal wave and  $\sigma$  is the

standard deviation of the Gaussian. If the resultant value of a point falls below a threshold, it belongs to an eyelash. This can be stated as:

$$f(x) * G(v, u, \sigma) < K_1 \quad (2)$$

where  $K_1$  is a pre-determined threshold and  $*$  is the convolution operator. The success of this process depends on a high intensity difference between iris pixels and eyelash pixels. Multiple eyelashes are modelled using an intensity variation model - eyelashes overlapping in a small area have a low intensity variation. If the variance of intensity in the area is below a threshold, the center of the window is labelled an eyelash pixel. This can be stated as:

$$\frac{\sum_{i=-N}^N \sum_{j=-N}^N (f(x+i, y+j) - M)^2}{(2N+1)^2} < K_2 \quad (3)$$

where  $M$  is the mean intensity in the window and  $(2N+1)^2$  is the window size and  $K_2$  is a threshold. A connected components algorithm is also implemented to avoid misclassification of pixels.  $K_1$  and  $K_2$  are empirically determined parameters.

The frequency distribution of iris images has been analyzed to determine occlusions by eyelids and eyelashes [17]. While effective, the technique does not provide a solution to removing the useless regions. In section 4 we discuss four methods for characterizing different parts of an iris image.

### 3. Preprocessing

Segmentation of the iris from an image of the eye is sensitive to numerous factors - noise, uneven lighting and eyelid and eyelash interference. Although the pupil and iris borders can be modelled using two non-concentric circles, with the larger one forming a closed contour around the smaller one, detection of these two boundaries is not a simple problem. In a typical case, the outer iris boundary is a very soft gradient that standard edge functions do not detect. This boundary is sometimes only partially visible or, possibly, covered by eyelash. Once localized, the iris is transformed into a  $544 \times 96$  grid to make it invariant to changes in pupil diameter. The details of the algorithm can be found in [18]. An example of a localized iris and a normalized one is shown in Fig. 1.

## 4. Texture Analysis

### 4.1. Gabor texture features

The Gabor function [19] is used to filter an image at different frequencies and orientations. The filter outputs reflect the spatial and orientation composition of a texture. It has the following form

$$g(x, y) = \exp\left\{-\frac{1}{2}\left(\frac{x^2}{\sigma_x^2} + \frac{y^2}{\sigma_y^2}\right)\right\} \cos\left(\frac{2\pi}{\lambda}x + \phi\right) \quad (4)$$

The  $x$  and  $y$  coordinates can be rotated spatially by a value  $\theta$  to produce a filter for different orientations. It can be performed by computing

$$x' = (x - \xi) \cos \theta + (y - \eta) \sin \theta \quad (5)$$

$$y' = -(x - \xi) \sin \theta + (y - \eta) \cos \theta \quad (6)$$

and substituting these values for  $x$  and  $y$ . The parameter  $\phi$  controls the phase offset of the function. We also have

$$\sigma_x = \frac{\sqrt{\ln 2}(2^{B_f} + 1)}{\frac{\sqrt{2\pi}}{\lambda}(2^{B_f} - 1)} \quad (7)$$

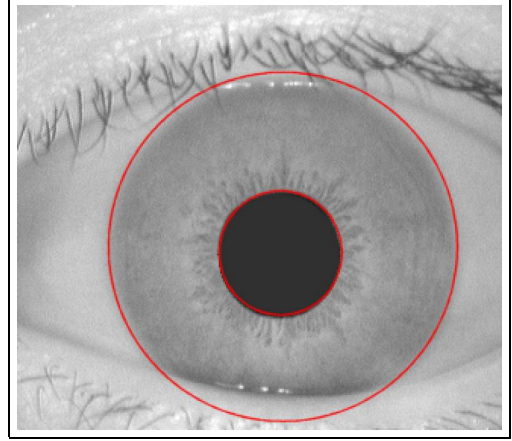


Figure 1: A localized iris and a normalized iris

$$\sigma_y = \frac{\sqrt{\ln 2}}{\frac{\sqrt{2\pi}}{\lambda} \tan\left(\frac{B_\theta}{2}\right)} \quad (8)$$

The frequency of the sinusoids is  $\frac{1}{\lambda}$ . The spread of the Gaussian in the  $x$  and  $y$  directions is controlled by  $\sigma_x$  and  $\sigma_y$  respectively. The frequency bandwidth of the filter is represented by  $B_f$  and the angular bandwidth by  $B_\theta$ .  $B_f$  is set to 1 (octave) and  $B_\theta$  is 30 degrees.  $\phi$  is set to 0 to create a symmetric filter and  $-\frac{\pi}{2}$  for an anti-symmetric filter. We compute the Gabor energy of an image by combining the outputs  $r$  of a symmetric (even) and anti-symmetric (odd) filter to establish a feature

$$f_{\lambda, \theta} = \sqrt{(r_{\text{even}})^2 + (r_{\text{odd}})^2} \quad (9)$$

for a particular  $\lambda$  and  $\theta$ . We use  $\theta \in \{0, 30, 60, 90, 120, 150\}$  and  $\lambda \in \{1, 1.41, 2.82\}$  and a maximum kernel size of  $9 \times 9$ .

### 4.2. The Discrete Wavelet Transform

A fundamental development in signal processing was that of the wavelet. Mallat [20] was the first to show that wavelets formed a powerful basis for multiresolution theory. Multiresolution theory incorporates ideas from subband coding, quadrature filters and pyramidal image processing. The DWT separates a signal into different frequency components and can be computed using a cascade of filters. Outputs for the filters  $h$  (high pass) and  $l$  (low pass) in the 1D case are given by:

$$a_{j+1}(x) = \sum_{n=-\infty}^{+\infty} l(n-2x)a_j(n) \quad (10)$$

$$d_{j+1}(x) = \sum_{n=-\infty}^{+\infty} h(n-2x)a_j(n) \quad (11)$$

The  $a_j$  represent the approximated signal and are used for the next scale of the transform while the  $d_j$  are the wavelet coefficients. At scale  $j+1$  there are half the number of elements as scale  $j$ . The DWT can be performed until only 2 elements remain.

Features computed from the wavelet coefficients are:

$$\mu = \frac{1}{N^2} \sum_{i=1}^N p(i) \quad (12)$$

$$e = \frac{1}{N^2} \sum_{i=1}^N [p(i)]^2 \quad (13)$$

$$\text{AAD} = \frac{1}{N^2} \sum_{i=1}^N |p(i) - \mu| \quad (14)$$

which are the mean, energy and absolute average deviation respectively. The filtered signal is represented by  $p$  while  $N$  is the number of elements in the signal. A generalized Haar [20, 21] algorithm decomposes the image, extracting detail and approximation coefficients. To perform feature extraction, a  $8 \times 8$  window is centered at each pixel and 2 passes of the Haar algorithm is performed on windowed pixels together with computation of the statistical information. At each scale, 4 sub-images are produced from the detail and approximation coefficients -  $LL$ ,  $LH$ ,  $HL$  and  $HH$ . Features are computed for  $LL$ ,  $LH$  and  $HH$ . For  $LL$ , the mean and AAD are computed. For  $LH$  and  $HL$ , the energy is computed. Thus, for each pass, 4 features are computed. In addition, the mean and AAD are computed for the original image. This provides a total of 10 features for the DWT transform of a texture.

#### 4.3. Co-occurrence Features

Haralick *et al.* [22] co-occurrence features are a popular and effective texture descriptor. It estimates the image properties to second-order statistical features. A GLCM (Grey Level Co-occurrence Matrix) element  $p_{\theta,d}(i, j)$  is the joint probability of the grey level pairs  $i$  and  $j$  in a given direction  $\theta$  separated by distance of  $d$  pixels. Three texture measures are computed from GLCMs generated from the input image. They are:

$$\text{CONT} = \sum_{i,j=1}^N (i-j)^2 p_{\theta,d}(i, j) \quad (15)$$

$$\text{ENTR} = - \sum_{i,j=1}^N p_{\theta,d}(i, j) \log p_{\theta,d}(i, j) \quad (16)$$

$$\text{MEAN} = \mu = \mu_x = \sum_{i,j=1}^N iP_x(i, j) \quad (17)$$

where

$$P_x(i) = \sum_{j=1}^N p_{\theta,d}(i, j) \quad (18)$$

In addition, a new feature has been defined:

$$\text{F1} = \sum_{i,j=1}^N p_{\theta,d}(i, j) \frac{i}{j} \quad (19)$$

Evidence is provided in [23] that GLCM texture features perform differently for particular images. Their work was consistent with previous works that divided GLCM features into 3 groups:

1. The contrast group - contrast, dissimilarity and homogeneity
2. The orderliness group - energy and entropy

3. Descriptive statistics - mean, standard deviation and correlation

and suggested combining one feature from group 1, one from group 2 and one or two from group 3. Group 1 and 2 have their members strongly correlated with the others in their group. We have selected one from each group and introduced a new feature. Features are computed for a  $9 \times 9$  window with the number of grey levels quantized to 64.

#### 4.4. Markov Random Fields

One of the most common and popular of the model-based approaches is the use of random fields. Markov Random Fields (MRF) construct a texture model by expressing all grey values in an image as a function of the grey values in a neighborhood of each pixel. A Markov random field [24] is a 2D lattice of points where each point is assigned a value that is influenced by its particular neighbouring values. Let  $X(i, j)$  be a random variable which denotes the grey value at site (pixel)  $(i, j)$  on an  $N \times M$  image lattice  $L$ . For simplicity,  $X$  shall be indexed with only one variable:  $X(c)$  where  $c = 1, 2, 3, \dots, N \times M$ . If  $y$  is a neighbour of  $x$  then  $\rho(X(x))$  depends on the value  $X(y)$ . Then the Markov random field is a joint probability density on the set of all digital numbers of  $L$  such that  $\rho(X(c)) > 0$  and

$$\rho(X(c) | X(m), m = 1, 2, 3, \dots, N \times M, c \neq m) = \rho(X(c) | \text{neighbours of } c) \quad (20)$$

A symmetric difference equation is used to model the Markov process for textures [25]:

$$X(c) = \sum \beta_{c,m} [X(c+m) + X(c-m)] + e_c \quad (21)$$

where the  $m_i$  is an offset to a neighbouring site. This is a Gaussian Markov Random Field (GMRF). Zero mean Gaussian distributed noise (estimation error) is denoted by  $e_c$ ,  $m$  is an offset from the center cell  $c$  and  $\beta_{c,m}$  are parameters that weigh a pair of symmetric neighbours to the center cell. The  $\beta$ s form the feature vector that describes the Markovian properties of the texture and govern the spatial interactions. A region  $R$  of size  $w \times w$  is defined together with the order of neighbourhood ( $N$ ). For every  $w_{ij}$  pixel in  $R$ , its neighbouring pixels up to order  $N$  describe a spatial interaction with the pixel. These spatial interactions for all  $w_{ij}$ s in  $R$  are modelled using the Gauss model described above. We can represent the equation in matrix notation:

$$X(c) = \beta^T \mathbf{Q}_c + e_c \quad (22)$$

$\beta$  is a vector consisting of all the  $\beta_{c,m}$  and  $\mathbf{Q}_c$  is a vector defined by:

$$\mathbf{Q}_c = \begin{bmatrix} X(c+m_1) + X(c-m_1) \\ X(c+m_2) + X(c-m_2) \\ X(c+m_3) + X(c-m_3) \\ \dots \end{bmatrix} \quad (23)$$

The  $\beta$ s can be estimated using a least squares approach:

$$\beta = \left[ \sum_{c \in N} \mathbf{Q}_c \mathbf{Q}_c^T \right]^{-1} \left[ \sum_{c \in N} \mathbf{Q}_c X(c) \right] \quad (24)$$

Features are computed using the  $\beta$ s by a modified method presented in [26]. The neighbourhood order is 5 ( $5 \times 5$  window) with a smoothing window of  $5 \times 5$ . The region  $R$  is  $9 \times 9$ . Prior to computing the texture features, the intensity image must be transformed to a zero mean image. To do this, for every pixel

$x_{ij}$  in the intensity image, compute a local mean  $\mu$  in a windowed region centered at  $x_{ij}$ . Then the new value of  $x_{ij}$  in the zero mean image is  $x_{ij} - \mu$ .

## 5. Unsupervised Pattern Classification

The segmentation of an iris image is a problem of unsupervised classification. In essence, we are required to partition the set of feature vectors into classes that differ from each other as much as possible. Concurrently, the vectors in the same class must differ as little as possible. The number of distinct texture classes in the region of interest is unknown. Ideally, we require a two class classifier that separates iris texture and *any* other textures. The K-means [27] and fuzzy C-means [28] algorithms are implemented. There are a multitude of textures possible when an image of the eye is captured - skin, eyelash, sclera, iris and pupil. The texture variations are random due to uneven illumination, eyelashes and the state of the pupil.

### 5.1. K-means Clustering

The MacQueens  $k$ -means algorithm is a popular clustering algorithm in which the number of clusters ( $k$ ) is known. It is an iterative process that assigns patterns to the closest cluster using a distance function (such as the Euclidean distance measure). The basic algorithm is described below.

1. Define the number of clusters  $k$ .
2. Initialize (randomly) the clusters prototypes  $\mathbf{p}_i$  ( $i = 1..k$ ).
3. For each pattern  $\mathbf{x}$ , assign  $\mathbf{x}$  to the nearest cluster  $\mathbf{p}_i$  ( $i = 1..k$ ).
4. Recompute  $\mathbf{p}_i$  ( $i = 1..k$ ).
5. Repeat steps 3 and 4 until the prototypes do not change.

The algorithm we use is similar to the once described above but uses a function to derive weights for the distance function. The weighting function is proposed in [29].

### 5.2. Fuzzy C-means Clustering

Fuzzy clustering allows data to belong to more than one class. This is reflected by their degree of membership in a particular cluster. It is based on the minimization of the objective function

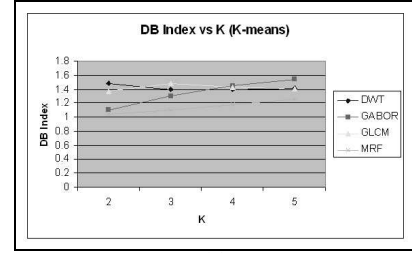
$$J_m = \sum_{i=1}^N \sum_{j=1}^C u_{ij}^m \| \mathbf{x}_i - \mathbf{v}_j \|^2, \quad 1 \leq m \leq \infty \quad (25)$$

where  $m$  is a real number greater than 1 (called the fuzzification factor).  $u_{ij}$  is the degree of membership of  $\mathbf{x}_i$  in the cluster  $j$  where  $0 \leq u_{ij} \leq 1$ .  $\mathbf{x}_i$  is the  $i^{th}$  component in a  $d$ -dimensional data set (vectors).  $\mathbf{v}_j$  is the  $d$ -dimension center of cluster  $j$  and  $\| * \|$  is the Euclidean norm.  $C$  denotes the number of clusters and  $N$  the number of pattern vectors. Fuzzy partitioning is an iterative optimization process. The degree of membership ( $u_{ij}$ ) and the cluster centers  $\mathbf{v}_j$  are computed by the following equation:

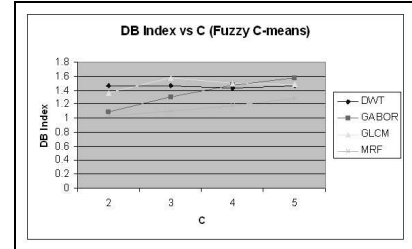
$$u_{ij} = \frac{1}{\sum_{k=1}^C \left( \frac{\|\mathbf{x}_i - \mathbf{v}_j\|}{\|\mathbf{x}_i - \mathbf{v}_k\|} \right)^{\frac{2}{m-1}}} \quad (26)$$

$$\mathbf{v}_j = \frac{\sum_{i=1}^N u_{ij}^m \cdot \mathbf{x}_i}{\sum_{i=1}^N u_{ij}^m} \quad (27)$$

The stopping criterion is  $|u_{ij}^k - u_{ij}^{k-1}| < \epsilon$ , where  $\epsilon$  is a threshold between zero and one. The algorithm is as follows:



(a)



(b)

Figure 2: a) DB index for k-means b) DB index for fuzzy c-means

1. Select the values of  $\epsilon$  and  $c$  and initialize the counter  $k$  to 0 ( $k \leftarrow 0$ ).
2. Obtain (randomly) the initial membership matrix,  $U^{(0)}$ .
3.  $k \leftarrow k + 1$
4. Compute the centroids  $\mathbf{v}_j$  ( $j = 1, \dots, c$ ) using equation (7).
5. Compute the membership matrix  $U^{(k)}$  using equation (6).
6. If  $\|U^{(k)} - U^{(k-1)}\| < \epsilon$  then stop else go to step 3.

## 6. Experimental Results and Discussion

The first experiment conducted entailed using the Davies-Bouldin (DB) index [30] to study the trend of cluster separation as the number of classes increased and the separation indices for the different texture methods. The DB index aims to identify sets of clusters that are compact and well separated - the lower the index value the better the number of classes used for clustering. All feature sets were normalized to unit variance and zero mean. The DB index was computed for 104 test images with number of clusters from 2 to 5. This was done for the 4 texture analysis methods and the 2 clustering algorithms. The average DB index was then computed for each number of clusters. Table 1. shows the average DB indices for the different methods and parameters. Figure 2. shows the DB index curve as the number of clusters varies for k-means and fuzzy c-means. We can see that the DWT and GLCM indices are stable as the number of clusters increases while the MRF and Gabor indices keep increasing as the number of classes increases. This indicates that the Gabor and MRF features do not provide good separability as the number of clusters increases while the DWT and GLCM cluster separation remain fairly stable. In addition, the table of indices shows that the DB index for k-means is significantly lower than fuzzy c-means implying a better cluster separation by k-means clustering.

Clusters	K - means				Fuzzy C-means			
	2	3	4	5	2	3	4	5
DWT	1.488522	1.395825	1.393057	1.413366	1.466079	1.468112	1.425302	1.464433
GABOR	1.105371	1.299476	1.454863	1.541762	1.095002	1.30563	1.471374	1.576659
GLCM	1.37544	1.480828	1.42442	1.402535	1.364528	1.579542	1.494266	1.488112
MRF	1.041113	1.102439	1.176117	1.260792	1.036663	1.102858	1.1801	1.277371

Table 1: Average DB indices

We then performed a subjective evaluation on 50 test images to study the segmentation results. We set the number of classes to 2 for the clustering algorithms. The test images consisted of iris images with combinations of the following artifacts:

- pupillary border
- multiple eyelashes
- single eyelashes
- no eyelashes
- reflection
- uneven illumination
- physiological characteristics such as freckles

Figure 3. shows a few test results. The k-means algorithm is able to classify reflections, eyelashes and pupillary border pixels into a single cluster. Skin and iris texture form the second cluster. A supervised approach would be able to decompose this cluster into skin and iris pixels. The fuzzy c-means algorithm effectively separates iris and skin from eyelashes, reflection and pupillary border pixels. However, it also tends to classify freckles and other texture variations as belonging to non-iris pixels. If the  $k$  value for k-means is set to 3, the freckles are detected. This shows that k-means differentiates better between iris and non-iris pixels since freckles are classified as iris pixels, which is correct. Eyelashes at the lower eyelid are not located by the clustering algorithms. The reason for this is that these eyelashes are very fine and that the smoothing process in the preprocessing stage removes them.

The DWT performs the best from the 4 texture techniques. The segmentation boundaries are clear and precise. Freckles and other iris characteristics are not misclassified by the k-means clustering. It is able to generalize well in uneven illumination. The non-iris pixels correspond to high energies with various fluctuations.

The GLCM method has the ability to clearly distinguish eyelash zones. The new feature proposed produces a high response in the presence of eyelashes and reflections and the pupillary border. When the gradient between different zones is low, the algorithm fails to detect the transition although the segmentation result is acceptable. The technique is not sensitive to small noisy fluctuations in texture. It also produces precise and unbroken segmentation contours.

The Gabor filters are very promising. However, they are very sensitive to noise due to the small size of the kernels and the high frequency selectivity of the filter. A broader range of parameters can be used but segmentation accuracy would decrease. The dimensionality and running time would also be greatly affected. The filters are able to detect eyelashes effectively and with high precision due to its edge-like characteristics. The segmentation result contains jagged lines and edges

in some cases due to the sensitivity of the kernel to noise and fluctuations.

The MRF performs poorly in comparison to the other techniques. A high degree of misclassification occurs at some texture borders such as eyelash and iris. In some cases, zones are broken up. The features are not an accurate representation of texture areas.

Overall, we find that texture classification and unsupervised clustering is very promising for segmenting iris images. A supervised approach would greatly improve results.

## 7. Future Developments

A learning process will be performed to determine particular texture characteristics of different regions in an iris image. This will provide data for attaching labels to clusters so that regions can be identified correctly.

## 8. Conclusion

The results presented in this paper show a distinctive pattern difference between iris and non-iris texture that will assist in accurate segmentation of iris images. The DWT performs the best from the four texture techniques. The GLCM and Gabor filter features are also very promising. The MRF performs poorly for this application area in comparison to the other methods. The k-means clustering algorithm with weighted distance measure performs better than the fuzzy c-means algorithm.

## 9. Acknowledgement

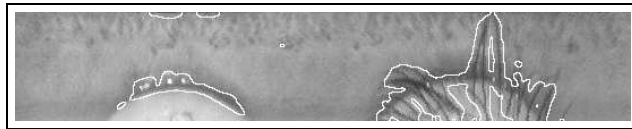
Portions of the research in this paper use the CASIA iris image database collected by the Institute of Automation, Chinese Academy of Sciences. The financial assistance of the National Research Foundation (NRF) towards this research is hereby acknowledged. Opinions expressed and conclusions arrived at are those of the authors and not necessarily to be attributed to the NRF. Armscor (SA) is also acknowledged for their financial support towards this project.

## 10. References

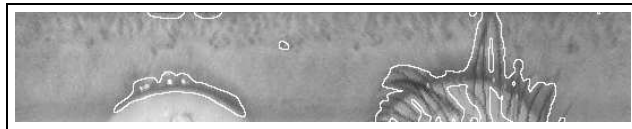
- [1] F.H. Adler, *Physiology of the eye*, MO: Mosby, St. Louis, 1965.
- [2] P.C. Kronfeld, "The gross embryology of the eye", *The Eye*, vol. 1, pp. 1–66, 1968.
- [3] L. Flom and A. Safir, "Iris recognition system", 1987.
- [4] H. Davson, *Davson's Physiology of the Eye*, MacMillan, London, 1990.
- [5] J. Daugman, "High confidence visual recognition of persons by a test of statistical independence", *IEEE Trans.*



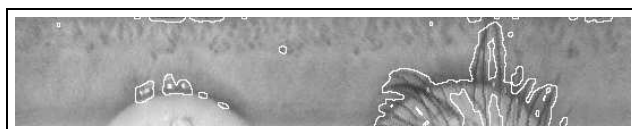
(a) Test image



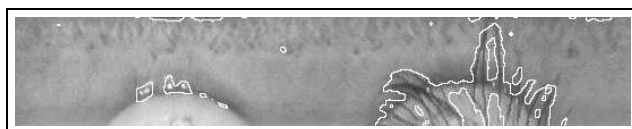
(b) DWT and k-means



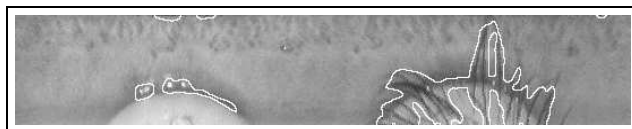
(c) DWT and fuzzy c-means



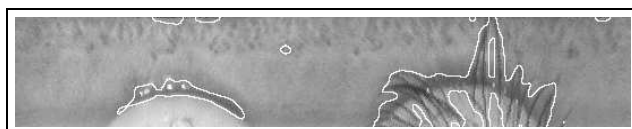
(d) Gabor and k-means



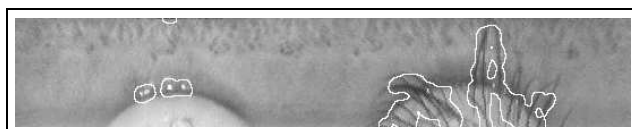
(e) Gabor and fuzzy c-means



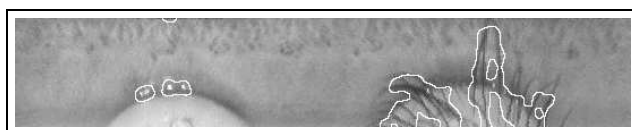
(f) GLCM and k-means



(g) GLCM and fuzzy c-means



(h) MRF and k-means



(i) MRF and fuzzy c-means

Figure 3: Some test results

on *Patt. Anal. and Mach. Intell.*, vol. 15, no. 11, pp. 1148–1961, 1993.

- [6] R.P. Wildes, “Iris recognition: an emerging biometric technology”, *Proceedings of the IEEE*, vol. 85, no. 9, pp. 1348–1362, 1997.
- [7] L.P. Boles and B. Boashash, “A human identification technique using images of the iris and wavelet transform”, *IEEE Trans. on Signal Processing*, vol. 46, no. 4, pp. 1185–1188, 1998.
- [8] J. Daugman, “The importance of being random: stastical principles of iris recognition”, *Pattern Recognition*, vol. 36, no. 2, pp. 279–291, 2003.
- [9] J.M.H. Ali and A.E. Hassanien, “An iris recognition system to enhance e-security environment based on wavelet theory”, *Advanced Modelling and Optimization*, vol. 5, no. 2.
- [10] K. Lim, K. Lee, O. Byeon and T. Kim, “Efficient iris recognition through improvement of feature vector and classifier”, *ETRI Journal*, vol. 23, no. 2, pp. 61–70, 2001.
- [11] K. Lim, Y. Wang and T. Tan, “Iris recognition based on multichannel gabor filtering”, in *Fifth Asian Conference on Computer Vision*, 2002, vol. 1, pp. 279–283.
- [12] Y. Wang L. Ma and T. Tan, “Iris recognition using circular symmetric filters”, in *ICPR*.
- [13] Y. Wang L. Ma, T. Tan and D. Zhang, “Efficient iris recognition by characterizing key local variations”, *IEEE Transactions on Image Processing*, vol. 13, no. 6, pp. 739–750, 2004.
- [14] C.H. Chen, L.F. Pau, and P.S.P. Wang, *The Handbook of Pattern Recognition and Computer Vision (2nd Edition)*, World Scientific Publishing Co., 1998.
- [15] B. Jahne, H. Haubecker, P. Geibler, *Handbook of Computer Vision and Applications - Volume 2*, Academic Press, 1999.
- [16] W.K. Kong and D. Zhang, “Detecting eyelash and reflection for accurate iris segmentation”, *International Journal of Pattern Recognition and Artificial Intelligence*, vol. 17, no. 6, pp. 1025–1034, 2003.
- [17] L. Ma, T. Tan, Y. Wang and D. Zhang, “Personal identification based on iris texture analysis”, *IEEE Trans. on Patt. Anal. and Mach. Intell.*, vol. 25, no. 12, pp. 1519–1533, 2003.
- [18] A.K. Bachoo and J-R. Tapamo, “A segmentation method to improve iris-based person identification”, in *Africon 2004*, 2004, vol. 1, pp. 403–408.
- [19] A.K. Jain, N.K. Ratha and S. Lakshmanan, “Object detection using gabor filters”, *Pattern Recognition*, vol. 30, no. 2, pp. 295–309, 1997.
- [20] Mallat S., “A theory of multiresolution signal decomposition”, *IEEE Trans. on Patt. Anal. and Mach. Intell.*, vol. 11, no. 7, pp. 674–693, 1989.
- [21] J.-L. Starck, F. Murtagh and A. Bijaoui, *Image Processing and Data Analysis: The Multiscale Approach*, Cambridge University Press, 1998.
- [22] R.M. Haralick, K. Shanmugam and I. Dinstein, “Texture features for image classification”, *IEEE Trans. System Man. Cybernat.*, vol. 8, no. 6, pp. 610–621, 1973.

- [23] Q. Zhang, J. Wang, P. Gong and P. Shi, "Study of urban spatial patterns from spot panchromatic imagery using textural analysis", *Int. J. Remote Sensing*, vol. 24, no. 21, pp. 4137–4160, 2003.
- [24] J. Besag, "Spatial interaction and the statistical analysis of lattice systems", *Journal of the Royal Statistical Society, series B*, vol. 36, no. 2, pp. 192–236, 1974.
- [25] J.W. Woods, "Two-dimensional discrete markovian fields", *IEEE Trans. Info. Theory*, vol. 18, no. 2, pp. 232–240, 1972.
- [26] E. Cesmeli and D. Wang, "Texture segmentation using gaussian-markov random fields and neural oscillator networks", *IEEE Trans. on Neural Networks*, vol. 12, no. 2, pp. 394–404, 2001.
- [27] J. MacQueen, "Some methods for classification and analysis of multivariate observations", 1967, pp. 281–297.
- [28] J.C. Dunn, "A fuzzy relative of the isodata process and its use in detecting compact well separated clusters", *Journal of Cybernetics*, vol. 3, pp. 32–57, 1974.
- [29] J.Z. Huang, M.K. Ng, H. Rong and Z. Li, "Automated variable weighting in k-means type clustering", *IEEE Trans. on Patt. Anal. and Mach. Intell.*, vol. 27, no. 5, pp. 657–668, 2005.
- [30] D.L. Davies and D.W. Bouldin, "A cluster separation measure", *IEEE Trans. on Patt. Rec. and Mach. Intell.*, vol. 1, no. 2, pp. 224–227, 1979.